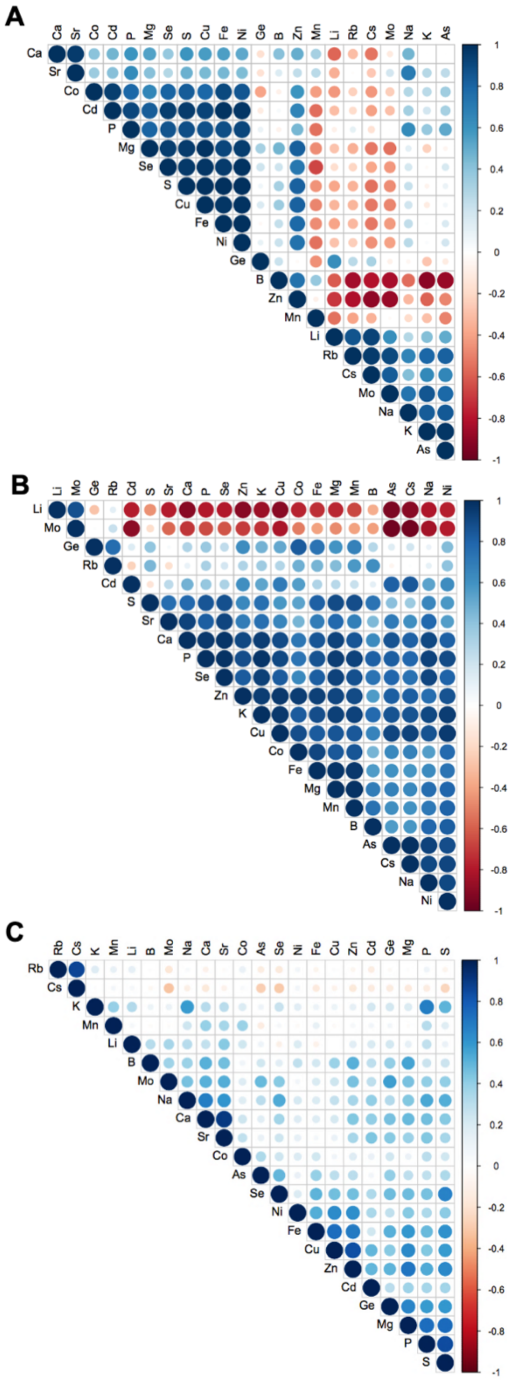

Supplementary Figure S1 Correlation matrix showing associations between elements measured in the 2020 growing season.
Elements were analyzed from grains and pairwise correlations conducted for (A) data obtained from 5 biological replicates of BTx623, (B) data obtained from 5 biological replicates of NOG and (C) 169 F_{13} RILs, using Pearson's correlation coefficients. Deep blue and deep red colors denote strong positive and negative correlations between elements, respectively. The size of the circles also indicates the strength of the correlation, with bigger circles indicating stronger correlation.

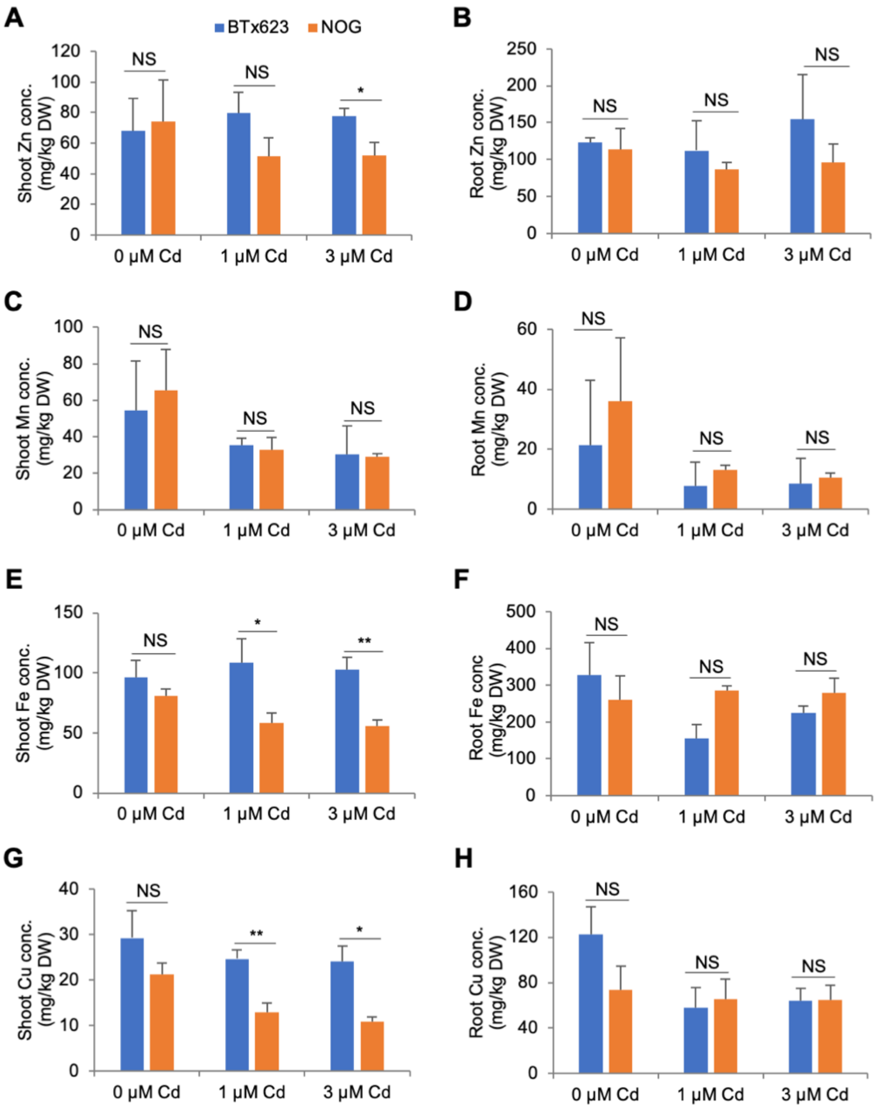

Supplementary Figure S2 Concentration of mineral elements in the shoots and roots of parental lines grown in various Cd concentrations.
Hydroponics experiments were conducted to analyze the shoot and root concentration of Cd and other elements in seedlings grown in different Cd treatments. (A), (C), (E), and (G) show the shoot concentrations, and (B), (D), (F), and (H) show the root concentrations of Zn, Mn, Fe and Cu in both BTx623 and NOG. Data are means ± SD of 3 biological replicates. * and ** denote significant differences at $P < 0.05$ and $P < 0.01$ respectively, calculated using Student's *t*-test, NS indicates not significant, DW grain dry weight.

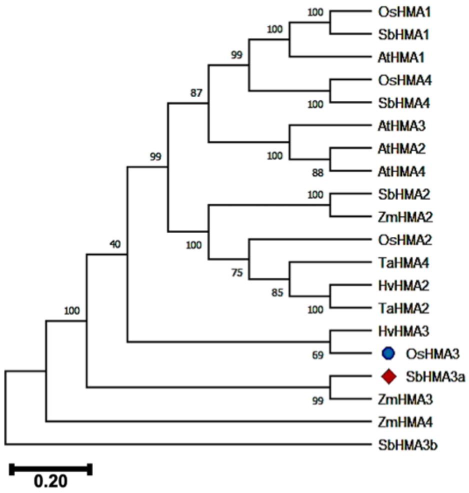

Supplementary Figure S3 Phylogenetic tree of HMA proteins from different plant species.
HMA peptides from rice, barley, maize, and *Arabidopsis thaliana* were obtained from their respective databases and used for phylogenetic tree construction using maximum likelihood method in MEGAX. Bootstrap values based on 1,000 replicates are shown at nodes in percentage.

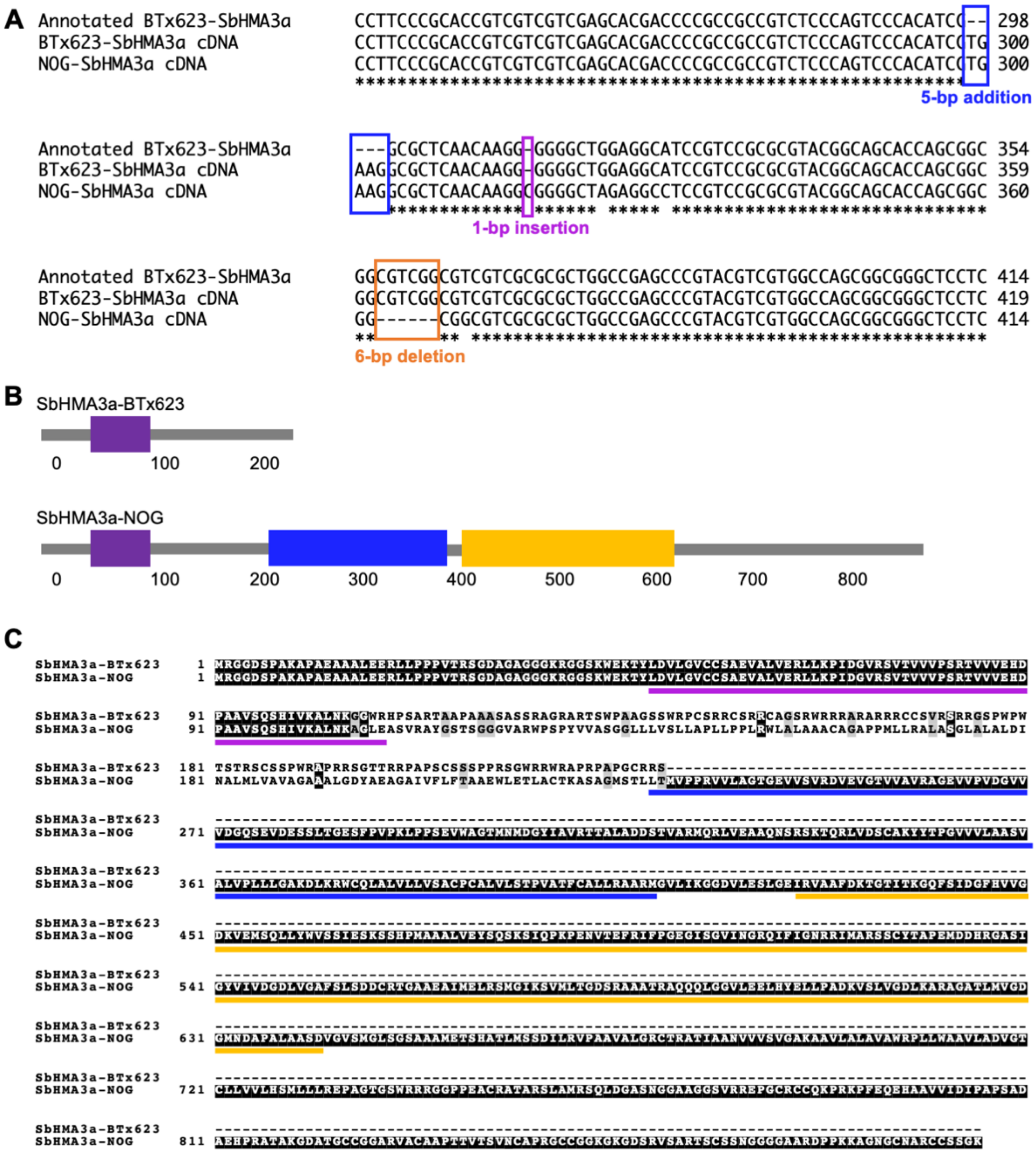

Supplementary Figure S4 Schematic illustration of predicted protein domains and nucleotide and peptide sequence alignments showing polymorphisms between *SbHMA3a-BTx623* and *SbHMA3a-NOG.*
(A) Nucleotide sequence alignments showing mutations observed in the cloned genes compared with the annotated sequence. The blue box shows the 5-bp addition in *SbHMA3a-BTx623* and *SbHMA3a-NOG* obtained from cloned and sequenced cDNA. The 1-bp insertion and 6-bp deletion in cloned *SbHMA3a-NOG*, are indicated by purple and orange boxes, respectively. Multiple alignment was done using ClustalW. (B) Upper panel; *SbHMA3a-BTx623* encodes a truncated peptide carrying only a HMA domain. Lower panel; *SbHMA3a-NOG* encodes a protein of 895 amino acids, carrying the conserved HMA, E1-E2 ATPase, and hydrolase domains of P_{1B}-type ATPases indicated in purple, blue and yellow bars respectively. Predictions were made using the SMART database (http://smart.embl-heidelberg.de/). (C) Peptide sequence alignment showing the HMA domain in both SbHMA3a-BTx623 and SbHMA3a-NOG indicated by a purple line, whereas the E1-E2 ATPase and hydrolase domains in SbHMA3a-NOG are indicated in blue and yellow lines, respectively. Alignment was done using Boxshade (https://embnet.vital-it.ch/software/BOX_form.html).

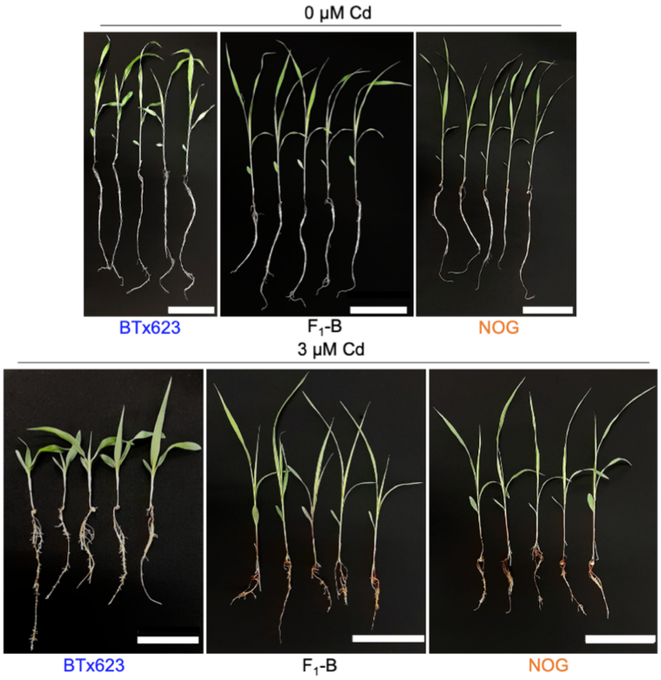

Supplementary Figure S5 Phenotypes of shoots and roots of parental lines and F_1 plants.
Seedlings were grown in the absence or presence of 3 μM Cd for 14 days. Scale bars indicate 5 cm.

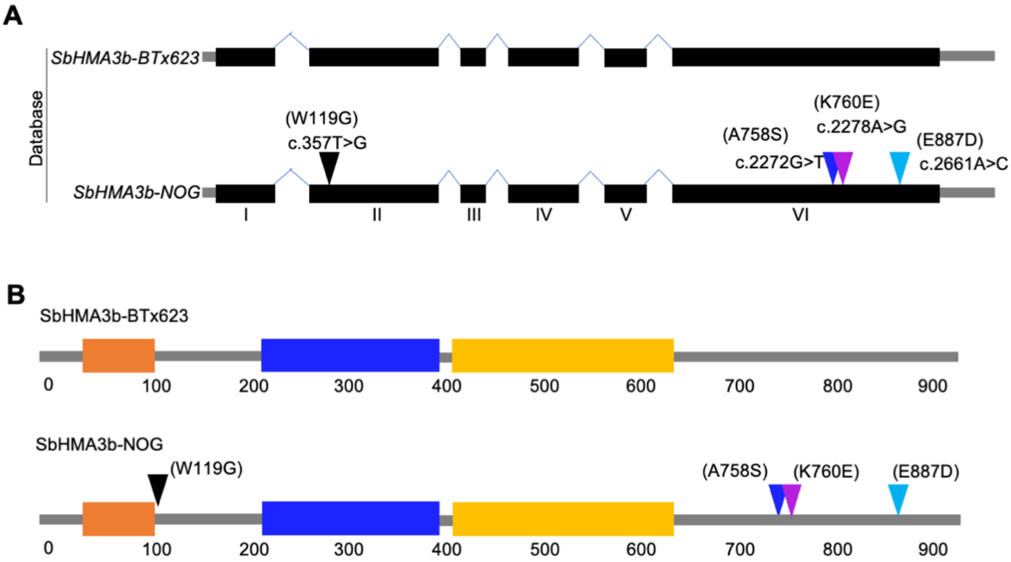

Supplementary Figure S6 Schematic representation of the annotated *SbHMA3b* from BTx623 and the corresponding gene in NOG and their peptide domains.
(A) The gene structure of *SbHMA3b-NOG* was constructed with that of BTx623 annotated in the Phytozome v13 database (https://phytozome-next.jgi.doe.gov/). Base and amino acid substitutions in NOG are shown. Black bars represent exons, gray bars show the 5' and 3' UTR regions, while hats represent introns. (B) The predicted protein domains of SbHMA3b-BTx623 (upper panel), and SbHMA3b-NOG (lower panel). Predictions were done using SMART database (http://smart.embl-heidelberg.de/). Base and amino acid substitutions in NOG are shown approximately. Orange bars represent a protein database domain 2KKH, E1-E2 ATPase and hydrolase domains, are shown in blue and yellow bars respectively.

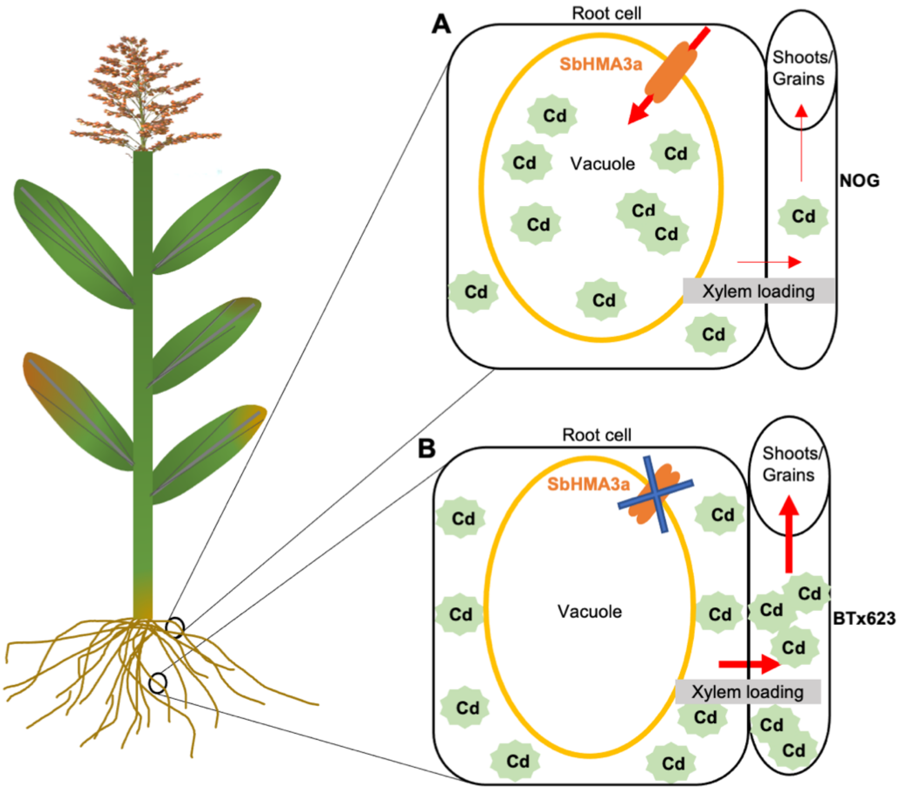

Supplementary Figure S7 Schematic proposed model of root to shoot translocation of Cd via *SbHMA3a.*
(A) Functional *SbHMA3a* sequesters Cd into the vacuole, reducing xylem loading and accumulation in above-ground tissue. (B) Loss of function of *SbHMA3a* permits xylem loading thus high accumulation in above-ground tissues and grains. The red arrows show the direction of Cd transport. Thickness of the arrows indicates relative amount of Cd transported.

Supplementary Table S1: Summary of identified QTLs for grain elements using the F_{12} and F_{13} RIL population.

QTL[a]	LOD score[a]	Nearest marker[a]	PVE (%)[a]	QTL[b]	LOD score[b]	Nearest marker[b]	PVE (%)[b]
qLi-19	3.5	Chr10.59656072	5.5				
qB-19	5.1	Chr01.27965371	8.8	*qB-20*	4.0	Chr04.62639493	5.6
	3.0	Chr04.58794505	6.1				
qNa-19	3.2	Chr04.62422347	7.7	*qNa-20*	3.6	Chr01.72086062	0.2
qMg-19	5.8	Chr03.16839921	5.6	*qMg-20*	3.1	Chr02.72696268	4.5
	3.7	Chr04.1039163	7.3				
qP-19	5.1	Chr09.10218273	6.3	*qP-20*	3.2	Chr01.70658868	6.2
					3.3	Chr10.55498177	4.7
qS-19	4.3	Chr07:11017179	7.7				
qK-19	3.1	Chr10.11967690	5.5	*qK-20*	3.1	Chr01.71093025	7.4
					4.0	Chr05.59432156	7.1
qCa-19	3.8	Chr03:2813486	7.5				
	3.0	Chr08:57258936	7.3				
qMn-19	5.2	Chr05.65846634	2.5	*qMn-20*	3.9	Chr02.57244774	5.1
	3.8	Chr09.50837916	5.5				
qFe-19	4.2	Chr07.62290676	6.3				
	3.8	Chr09.8279789	8.8				
				qNi-20	4.4	Chr06.53574620	5.9
				qCu-20	5.1	Chr08.3415305	3.0
qCo-19	4.9	Chr06.42574550	3.0				
qZn-19	5.7	Chr01.27269526	7.2	*qZn-20*	3.2	Chr01.2955610	6.5
					3.3	Chr08.5764378	5.1
qGe-19	4.7	Chr04.8104886	4.2	*qGe-20*	5.8	Chr02.65722873	9.8
					4.1	Chr06.47546161	7.3
qAs-19	3.3	Chr07.1164989	6.8	*qAs-20*	3.3	Chr05.65042029	3.8
qSe-19	6.1	Chr07.4122693	3.4	*qSe-20*	5.6	Chr02.65722873	8.4
qRb-19	4.0	Chr06.17737701	7.2	*qRb-20*	3.9	Chr02.65652401	6.5
	6.8	Chr09.56880571	12.1		3.1	Chr03.61989413	4.8
					5.6	Chr08.58019641	10.2
qSr-19	3.4	Chr03.2580521	6.1	*qSr-20*	4.2	Chr04.62016690	9.5
	3.2	Chr04.54110736	4.5				
qMo-19	3.5	Chr01.12925168	6.2	*qMo-20*	3.4	Chr02.65722873	5.1
	5.6	Chr04.64980399	10.7				
qCd-19	5.1	Chr01.25675981	3.0	*qCd-20*	**9.5**	Chr02.8937547	18.4
	24.5	Chr02.8937547	40.3				

LOD: Log of Odds with a threshold of 3, PVE: Percentage phenotypic variation explained. Highlighted LOD scores represent a LOD threshold based on a permutation test with 1,000 iterations.

[a] represents QTLs obtained in the F_{12} RIL population, and [b] represents QTLs obtained in the F_{13} RIL population. Empty cells show no QTLs were obtained for the particular elements.

Supplementary Table S2: List of annotated genes in the fine-mapped region of 156 kb *.

Location	Gene identifier	Description
Chr02:8852665-8853949	Sobic.002G082800.1	similar to Putative uncharacterized protein OSJNBa0086N05.106
Chr02:8868171-8871784	Sobic.002G082900	similar to Os07g0231400 protein
Chr02:8874038-8875484	Sobic.002G082950	no orthologues
Chr02:8878263-8881628	Sobic.002G083000	similar to Cation-transporting ATPase
Chr02:8884421-8888126	Sobic.002G083100	similar to Cation-transporting ATPase
Chr02:8889038-8893535	Sobic.002G083200	similar to Putative uncharacterized protein
Chr02:8902830-8908459	Sobic.002G083266.4	similar to Flavohemoprotein b5/b5R-like
Chr02:8909408-8912907	Sobic.002G083400.1	similar to Putative uncharacterized protein
Chr02:8914403-8917495	Sobic.002G083500.1	predicted protein
Chr02:8923187-8929483	Sobic.002G083600.1	similar to Putative indeterminate spikelet 1
Chr02:8936832-8939998	Sobic.002G083800	similar to Breast adenocarcinoma marker-like
Chr02:8942255-8952208	Sobic.002G083900	weakly similar to Chromosome chr6 scaffold_3, whole genome shotgun sequence
Chr02:8978190-8979235	Sobic.002G084100	No orthologues
Chr02:9001487-9001708	Sobic.002G084200.1	No orthologues
Chr02:9002326-9008005	Sobic.002G084300	similar to Ethylene-responsive small GTP-binding protein
Chr02:9008861-9014124	Sobic.002G084400	PF01535//PF13041//PF13812//PF14432 - PPR repeat (PPR) // PPR repeat family (PPR_2) // Pentatricopeptide repeat domain (PPR_3) // DYW family of nucleic acid deaminases (DYW_deaminase)
Chr02:9015131-9018185	Sobic.002G084500	similar to Os02g0279800 protein

* Data was obtained from Phytozome v13 database (https://phytozome-next.jgi.doe.gov/).

Supplementary Table S3: Primers used in this study.

Primer name	Sequence (5'-sequence-3')
G1-F	CCGGGTACCATGAGGGGTGGCGATAGCCCG
G1-R	CCGGGTACCTTATTTGCCACTAGAGCAAC
G1-RT F	CAGTCCCACATCGTGAAGG
G1-RT R	ACGGCTATGTAACCGTCCAT
EIF4a F	TGCTCTTGGGGACTATTTGG
EIF4a R	CTTGTCTGTGAGCCAGTCCA
PP2A F	TCCTCATGAAGGACCCATGT
PP2A R	AAAAAGTAGTCTGGGGTTTTGC

Supplementary Table S4: Gene ID numbers for HMA proteins used for phylogenetic analysis in this study.

Protein name	Gene ID
OsHMA1	Os06g0690700
OsHMA2	Os06g0700700
OsHMA3	Os07g0232900
OsHMA4	Os02g0196600
AtHMA1	AT4G37270
AtHMA2	AT4G30110
AtHMA3	AT4G30120
AtHMA4	AT2G19110
SbHMA1	Sobic.010G240500
SbHMA2	Sobic.010G250900
SbHMA3a	Sobic.002G083000
SbHMA3b	Sobic.002G083100
SbHMA4	Sobic.004G079900
ZmHMA2	Zm00001eb095010
ZmHMA3	Zm00001eb095020
ZmHMA4	Zm00001eb431150
TaHMA2	TraesCS7A02G419500
TaHMA4	TraesCS7A02G420000
HvHMA2	HORVU.MOREX.r3.5HG0509930
HvHMA3	HORVU.MOREX.r3.5HG0509930

Rice HMA gene IDs were obtained from Oryzabase (https://shigen.nig.ac.jp/rice/oryzabase/), *A. thaliana* gene IDs were obtained from TAIR (https://www.arabidopsis.org/index.jsp), Sorghum HMA IDs were obtained from Phytozome (https://phytozome-next.jgi.doe.gov/) while Maize, Wheat and Barley were obtained from *EnsemblPlants* (http://plants.ensembl.org/index.html).